Paramagnetic effect of the two-dimensional mixed state in type-I superconductors

I. L. Landau

Institute of Physics Problems, USSR Academy of Sciences
(Submitted February 1, 1974)
Zh. Eksp. Teor. Fiz. **67**, 250–262 (July 1974)

A new type of paramagnetic effect in hollow cylindrical single crystals of indium is observed and studied experimentally. It was found that as the superconductivity of such samples is destroyed by current in the presence of a longitudinal magnetic field, the magnitude of the longitudinal magnetic field in the sample aperature appreciably exceeds the external field. This is the case even for the current in the sample exceeding I_i, when practically the whole volume of the sample is in the normal state and all the differences of the sample behavior from that of the normal metal are brought about by a thin layer of the two-dimensional mixed state on its inner surface.

In this work a new type of paramagnetic effect was experimentally observed and studied in hollow cylindrical samples of type-I superconductors. It turned out that when superconductivity of such samples is destroyed by current in the presence of a longitudinal magnetic field, the magnitude of the magnetic field in the aperture of the sample is then appreciably larger than the external field even for currents much exceeding the critical value.

The paramagnetic susceptibility of samples in an intermediate state was first observed by Steiner and Schoeneck.[1] They studied solid cylindrical samples whose superconductivity was being destroyed by current in the presence of a longitudinal magnetic field. In this case the average magnetic permeability μ of the sample exceeds unity for a longitudinal field. The magnetic permeability of the sample has in this case a maximum at the current $I = I_c(H_e)$ (here $I_c(H_e)$ is the critical current through the sample in the longitudinal magnetic field of magnitude H_e). As the current increases the permeability decreases and for $I \gg I_c$ it tends to unity.

Similar phenomena were also observed later on in samples of other geometries, in particular in hollow cylinders (Meissner[2]). The study of the latter shape is of special interest, since in this case layers of a two-dimensional mixed state (TM state) of type-I superconductors are produced on the inner surface of a hollow cylindrical sample when its superconductivity is destroyed by current.[3-6]

The paramagnetic effect observed by Steiner and Schoeneck is associated with a peculiar structure of the intermediate state, which is produced in the presence of a longitudinal magnetic field as the superconductivity is being destroyed by current (see[3-6]). A similar effect in the hollow samples can therefore be observed only near the critical value of current at which there still exists a region of intermediate state in the sample. At the values of the current through the sample

$$I_0 > I_i = I_c(H_e)\,(r_1^2+r_2^2)/2r_1r_2$$

(r_1 and r_2 are respectively the inner and outer radii of the sample), the equilibrium diameter of the intermediate-state structure becomes smaller than the aperture diameter, and the whole sample is in the normal state apart from a thin TM layer on the inner surface.

These considerations fully agree with the experimental results obtained on hollow cylindrical samples. The magnetic permeability of the solid samples decreases gradually as the current increases, whereas in the hollow samples the permeability (and the magnetic field in the aperture) reaches a constant value already for currents exceeding the critical value by several percent.[2] It is also pointed out in[2] that at large currents through the sample the longitudinal magnetic field in the aperture is equal to the external field. The experiments described below show, however, that the longitudinal magnetic field in the sample aperture exceeds the external field even at currents that are above critical by a factor of tens. At currents slightly exceeding the critical value, the longitudinal magnetic field in the aperture is approximately twice as large as the external field (given $H_e \ll H_c$). It is hard to tell now why this effect was not detected on hollow cylinders made of mercury and tin.[2] Considerable inhomogeneity of the polycrystalline samples studied in[2] may be the explanation.

In the following we shall use the notation

$$H_c' = (H_c^2 - H_e^2)^{1/2}, \quad I_c' \equiv I_c(H_e) = {}^1/_2 c r_2 (H_c^2 - H_e^2)^{1/2}.$$

In other words H_c' and I_c' represent respectively the critical magnetic field (for a transverse field) and the critical current for a sample placed in a longitudinal magnetic field of magnitude H_e.

SAMPLE PREPARATION AND EXPERIMENTAL PROCEDURE

The samples on which the measurements were made were cast from indium with small admixture of tin. The resistance ratio R(300°K)/R(4.2°K) was equal to 1800 for the sample In1 and 2200 for In2. Both samples had the same size: 8 mm in outer diameter, 4 mm in inner diameter, and 55 mm in length. The fourfold axis of the crystal was in both cases parallel to the sample axis.

The mould for casting the samples is shown schematically in Fig. 1. A duraluminum insert 4 was placed inside a glass pipe 2 with polished inside surface. The pipe and the insert were prepared in such a way that at the melting temperature of indium (156°C) the thick ends of the insert would closely fit the pipe (this corresponds to a clearance of 0.02 mm at room temperature). The metal was poured into the clearance between the pipe sides and the insert through grooves 6. After the sample had been grown, the insert was dissolved in a hot caustic alkali solution which has practically no interaction with indium. The insert had an opening to facilitate its dissolution. During the sample casting this opening could be plugged with duraluminum.

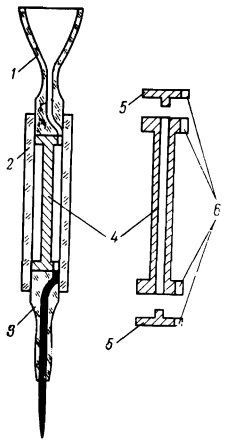

FIG. 1

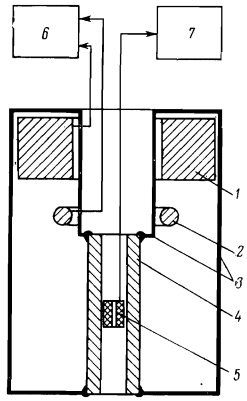

FIG. 2

FIG. 1. Mold for casting samples: 1—pouring channel, 2—mold, 3—primer, 4—duraluminum insert, 5—plugs, 6—grooves for pouring metal.

FIG. 2. Diagram of experimental: 1—core of superconducting transformer, 2—pickup of current meter, 3—lead-metal current leads, 4—sample, 5—fluxmeter coil, 6—current meter, 7—F-18 microwebermeter.

The samples were grown in a 10^{-5} Torr vacuum produced by a zeolite getter pump with a liquid nitrogen cooling.

To produce a current on the order of hundreds of amperes through the sample we used a transformer with superconducting windings (Fig. 2). The primary winding consisting of 200 turns of 50NT wire was wound on a toroidal soft-steel core 1. Circuit 3 (metallic lead) in series with sample 4 formed the secondary winding. A change in the current in the primary winding induced a voltage $V = -c^{-1}d\Phi/dt$ in the secondary winding ($d\Phi/dt$ is the rate of change of the magnetic flux through the transformer core). The considerable size of the steel core (2 cm in inner diameter, 7 cm in outer diameter, and 8 cm in height) allowed us to obtain currents as high as 500—800 A for several minutes even through our samples, which had rather large residual resistance.

The lead current leads were axially symmetric. The sample was welded to the leads by Wood's alloy; an experiment has shown that the resistance of such a contact is sufficiently small (less than 10^{-8} Ω at 500 A and 4.2°K).

The current in the sample was determined by measuring its magnetic field, by using a circular magnetic field indicator made of permalloy (see [10]). A diagram of the current meter is shown in Fig. 3. Three coils are wound on permalloy rings 2. The windings 3 and 4 form a normal transformer. The magnetizing winding 3 was wound on both rings oppositely directed. A sinusoidal voltage of frequency ν = 500 Hz was fed to it from the generator G. When no external circular magnetic field passes through the rings the signal in the secondary winding 4 is symmetric, i.e., it possesses no even harmonics. The appearance of a constant circular magnetic field on the rings violates the symmetry of their magnetic properties and a second-harmonic voltage is induced in the secondary winding (2ν), its phase being determined by the direction of the external field. The described device is a highly sensitive null-indicator of circular magnetic field, since premalloy reaches magnetic saturation in very weak fields. The oppositely directed connection of the magnetizing windings on the two rings enables us to substantially reduce the fundamental frequency signal and thus enhance the indicator's sensitivity.

The current I that we measured passed along the axis of the rings. Its magnetic field on the rings could be cancelled by passing direct current through a special compensating coil 1 of the current pickup. This coil was wound on both rings and consisted of 500 turns of superconducting wire 50 NT. The measured current I is equal to the current in the compensating coil at the instant of compensation, times the number of turns in the winding.

The indicator permalloy rings were cut from a foil 0.5 mm thick; the ring diameter was 30 mm, the width 3 mm. After manufacture, the rings were annealed in hydrogen for several hours at 1000°C.

An automatic measuring device was set up for convenience. Its block diagram is shown in Fig. 3. The voltage from the secondary winding of the pickup feeds the resonant amplifier A tuned to the frequency 2ν = 1000 Hz. The amplified signal is rectified by synchronous detector SD, and the dc voltage is then fed to a controlled-current source CCS, the output of which was connected to the compensating coil current pickup. Thus, this device automatically keeps the circular magnetic field on the pickup close to zero. It works with accuracy ~0.3% for currents ranging from several to several thousand amperes.

In conjunction with the superconducting transformer, the current meter could operate in one of two modes: swept current or constant current. In the first mode the primary current of the superconducting transformer of Fig. 2 varied smoothly with time, and the sample current was measured automatically. In the second mode a dc current was passed through the compensating coil of the current pickup (1 in Fig. 3). The output of CCS was fed to the primary winding of the superconducting transformer. The primary current was changed automatically to keep the sample current constant. The accuracy of current stabilization in this case was again ~0.3%.

In some of our experiments there was a conductor running along the sample axis. Current could be passed through this conductor independently of the sample current. A diagram of this experiment is shown in Fig. 4. A niobium cylinder of 3 mm diameter served as the central conductor 3; the conductor was centered in the sample aperture with the help of two duraluminum washers 4. The all-superconducting circuit of the central

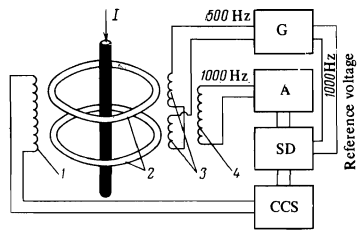

FIG. 3

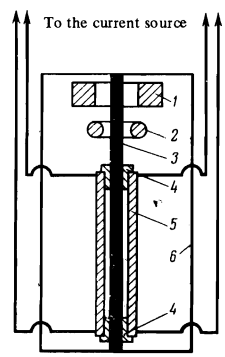

FIG. 4

FIG. 3. Diagram of current meter: 1—compensating coil, 2—permalloy rings, 3—magneting winding, 4—secondary winding; G—sine-wave generator, A—tuned amplifier, SD—synchronous detector, CCS—controlled current source.

FIG. 4. Diagram of experiment with central conductor: 1—core of superconducting transformer, 2—current meter, 3—central wire, 4—centering washers, 5—sample, 6—superconducting circuit of the transformer.

conductor wire was completed by strips of niobium foil 6 spot-welded to the niobium cylinder. Current in the conductor was fed from superconducting transformer 1 and was measured with the described current meter 2. The cross-section area of the transformer toroidal core was in this case about 3 cm^2. The current through the sample came from a bank of storage batteries; it was regulated with an emitter follower made up of sixteen P210 transistors. The maximum current of the circuit was about 200 A.

The longitudinal magnetic field on the sample was generated by a single-layer superconducting solenoid of 45 mm length, wound on a stainless steel tube of 11 mm diameter. We could also produce a transverse field on the sample with the aid of two mutually perpendicular pairs of Helmholtz coils; they were located directly inside a lead shell which served as the outer current conductor to the sample (3 in Fig. 2).

The longitudinal magnetic field in the sample aperture was measured by an F18 microweber meter with a coil 5 (Fig. 2) serving as its magnetic-field pickup. The coil consisted of several thousand turns of copper wire of 20 μm diameter, and had a length of 5 mm along the sample axis. We measured the signal of the microweber meter following reversal of the current in the solenoid. In the experiments with the central conductor it was practically impossible to place a coil in the sample aperture. Therefore, in these experiments the longitudinal magnetic field was determined by measuring the resistance of a thin bismuth wire (50 μm dia) positioned in the clearance between the central wire and the inner surface of the sample. The calibration curves of this field-strength meter were plotted at a temperature above the critical one of the sample ($T_c = 3.4°K$) for various values of the central-conductor current.

In some experiments we measured the impedance of the inner and outer sample surfaces at frequencies of the order of a few megacycles. For this purpose coils of copper wire of 50 μm diameter were placed on both surfaces of the sample. The coils served as inductors for a radio-frequency oscillator; we measured the variation in the oscillator frequency, which is proportional to the variation of the imaginary part of surface impedance. The coils had the shape of a single-layer solenoid, their axes coincided with that of the sample, and their length along the sample was equal to 5 mm. The change in the oscillator frequency during the superconducting transition was of the order of several kilocycles.

Throughout all the experiments the earth's magnetic field was cancelled, with accuracy ~0.020 Oe, by two pairs of Helmholtz coils.

RESULTS OF EXPERIMENTS AND THEIR DISCUSSION

1. Paramagnetic effect under axial-symmetry conditions.

It might be well to emphasize that the geometry of our experiments (the sample not too long and a short solenoid for generating the longitudinal magnetic field) provided no means to study near-critical phenomena. At currents close to the critical value there exists in the sample a region of intermediate-state structure, and this would require a high degree of longitudinal-magnetic-field homogeneity over rather long distances. On the other hand, this geometry is quite suited for the study of phenomena associated with a thin TM-state layer. Therefore, all the measurements described below pertain to sample currents $I_0 > I_i$, at which no intermediate-state region is present.

Figure 5 (curve 1) shows the dependence of the longitudinal magnetic field H_i in the sample aperture on the external longitudinal field H_e, plotted in relative units. The course of the curves did not depend on temperature, and depended very weakly on the current through the sample. The longitudinal magnetic field in the sample aperture thus appreciably exceeds the external field over almost the whole range of values of the latter. It becomes comparable with H_e only at $H_e \sim H_c$. At $H_e/H_c \approx 0.65$, H_i drops sharply as H_e increases. This part of the curve $H_i(H_e)$ is also accompanied by a pronounced hysteresis.

The impedance of the inner surface of the sample was also measured under similar conditions. The results are represented in Fig. 6. It is seen that the singularities on the $H_i(H_e)$ curve (Fig. 5) correspond to the instant when a sharp increase of the surface impedance takes place (Fig. 6). At large values of the longitudinal magnetic field the impedance starts to oscillate as a function of time with a frequency 1 to 2 Hz (the curves of Fig. 6 were obtained with constant-speed scanning of the external field).

It has been shown [4] that the central-conductor geometry makes possible the production of a TM-state layer not only on the inner surface, but also on the outer surface and in the volume of the sample. Similar experiments with a central conductor in the presence of a longitudinal magnetic field were carried out in the present work. Figure 7 shows the dependence of the longitudinal magnetic field in the sample aperture on the central-conductor current; the current through the sample and the external magnetic field are fixed in this case. So long as the central conductor current $|I_b|$ is less than $I_c' r_1/r_2$, a TM-state layer is present on the inner surface of the sample and the longitudinal magnetic field in the aperture is larger than the external field. if $I_b < I_c' r_1/r_2$, the TM layer disappears and the whole sample passes into the normal state; naturally, in this case $H_i = H_e$. At $I_b > I_c' r_1/r_2$, the TM-state layer moves into the interior of the sample, as shown in [4]. It is interesting that in this case we again have $H_i = H_e$. At $I_b = -I_0 - I_c'$ a TM layer appears on the outer sample surface and remains there for the current range $-I_0 - I_c' < I_b < -I_0 + I_c'$; at $I_b > -I_0 + I_c'$ the TM-state layer disappears and the sample becomes normal throughout. In the case when the TM layer is on the outer sample surface, the magnetic field in the aperture is appreciably lower than the external field. The dependence of H_i/H_c on H_e/H_c was also taken for the latter case; this dependence is plotted in Fig. 5 (curve 2) for $I_b = 93$ A.

The existence of a TM-state layer on the outer sample surface at $-I_0 - I_c' < I_b < -I_0 + I_c'$ is borne out by the results of measuring the impedance of this surface. These are to be found in Fig. 7 too (curve b). At $I_b = -I_0 - I_c'$ the impedance of the outer sample surface is seen to decrease from its normal value up to the practically superconducting value. Then, as the layer disappears at $I_b = -I_0 + I_c'$ the impedance regains its value for the normal surface.

If the destruction of superconductivity in the sample is due to the magnetic field of the current through the central conductor and there is neither current in the sample nor an external magnetic field, we can estimate the precision of centering the conductor along the sample axis from the width of the transition curve (measured by

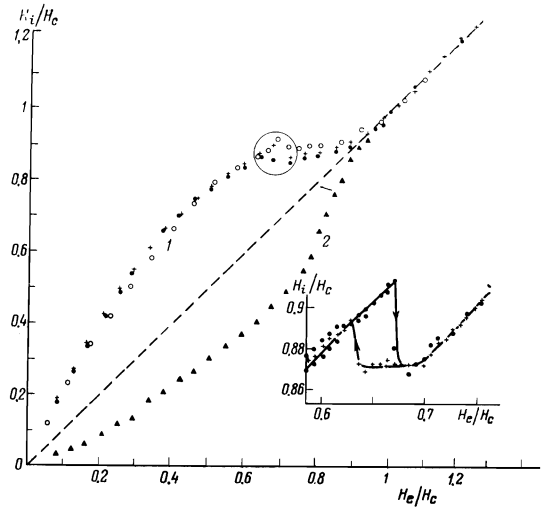

FIG. 5. Dependence of the longitudinal magnetic field in the sample aperture on the external field. Curve 1–TM-state layer on the inner surface of the sample ($I_b = 0$): ○–In1 sample, T = 3.194°K, $I_0 = 1.25\ I_c$ = 81 A; + and ●–In2 sample, T = 3.27°K, where + corresponds to I_0 = 1.25 I_c = 51 A, ● to I_0 = 2.08 I_c = 85 A. Curve 2–TM-state layer on the outer surface of the sample In2, $I_0 = -85$ A, $I_b = 93$ A, T = 3.27°K. The encircled region of the upper curve is magnified in the insert, sample In2, T = 3.194°K, $I_0 = 81$ A.

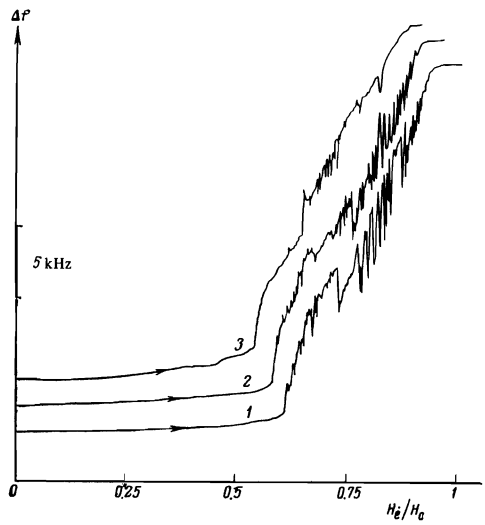

FIG. 6. Dependence of the inner surface impedance of the sample In2 on the longitudinal magnetic field, the oscillation frequency being 6.8 MHz, T = 3.375°K: 1–I_0 = 8.6 A, 2–I_0 = 15 A, 3–I_0 = 29 A; I_c = 6.6 A.

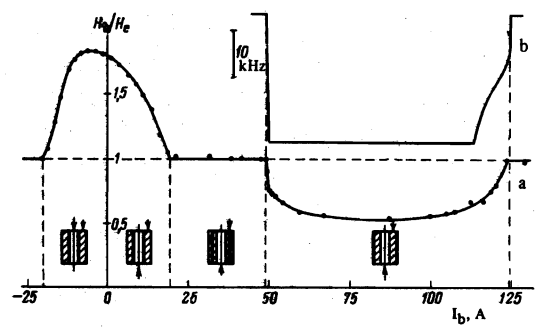

FIG. 7. a) Dependence of the longitudinal magnetic field in the aperture of the sample In2 on the current through the central wire; T = 3.27°K, $I_0 = -85$ A, $H_e = -0.4 \times H_c = 8.20$ Oe. The section of the sample is shown schematically below, the arrows indicate the current directions, the thick line shows the position of the TM-state layer. b) Impedance of the outer sample surface (ν = 5.5 MHz).

the surface impedance). Assuming that the transition-curve width in this case is determined by the non-coaxiality of the central conductor and the outer sample surface, we obtain the value 0.04 mm for this non-coaxiality.

Figure 8 shows the current dependences of the inner-surface impedance (Fig. 8a) and of the magnitude of the paramagnetic effect (Fig. 8b). It turns out that as the current increases the magnitude of the paramagnetic effect decreases almost linearly, and the paramagnetic effect vanishes near the current at which the impedance of the inner sample surface assumes its normal value.

As is known, the paramagnetic effect occurs also in type-II superconductors. In this case the paramagnetic effect is apparently brought about by the development of what is known as the force-free configuration of vortex filaments.[12] It is also conceivable that the paramagnetic effect of the TM-state layer arises from the presence of a vortex structure in the layer. Recently, however, another approach to the paramagnetic effect of the TM-state layer has been developed.

Andreev and Bestgen have developed a theory[6] of the TM state in the limit when the superconductivity of the layer is destroyed by current or by an electric field to such an extent that the formation of superconducting pairs in the layer can be regarded as fluctuations. Thus, this approximation is valid provided that $I_s \ll I_n$, where I_s and I_n are, respectively, the superconducting and the normal currents in the TM-state layer. Our samples being quite pure, this approximation holds only in an extremely narrow neighborhood of the critical current at which the TM state disappears completely.

On the other hand, we can imagine a type-I superconducting alloy with $\kappa \sim 1/\sqrt{2}$ and $l \sim \xi$; in such objects the theory is valid practically throughout the whole region of existence of the TM state. For this case, Bestgen[13] calculated the effect of a longitudinal magnetic field on a TM-state layer at $H_e \ll H_c$ and $I_0 \ll I_{c2}$, where I_{c2} is the current of total destruction of the TM-state layer (see[14]). All the results of these calculations agree with the experiment qualitatively, whereas a quantitative comparison of this theory with our experiments is impossible because both assumptions of the theory, $I_0 \ll I_{c2}$ and $I_s \ll I_n$, are never fulfilled simultaneously (for our samples $I_s \ll I_n$ only if $I_0 \sim I_{c2}$).

The results obtained in the experiments with the central conductor admit of the following physical interpretation. So long as the TM-state layer is located in the sample volume, it consists of two like parts, in one of which the circular magnetic field varies from $-H_c'$ to zero and in the other from zero to H_c' (the thickness of the layer being much smaller than its radius of curva-

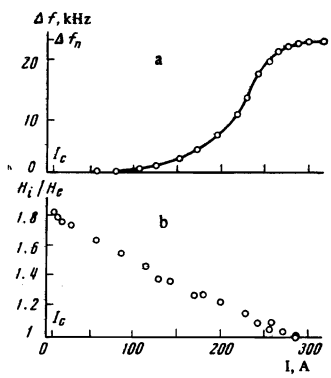

FIG. 8. Dependences of the current through the sample of a) inner surface impedance b) magnitude of paramagnetic effect. Sample In2, T = 3.375°K, H_e = 0.22 H_c = 0.73 Oe.

ture, we can neglect the effect of the curvature and regard the layer as locally flat). Application of the longitudinal magnetic field causes a helical twist of the current in the layer. The sign of the helix is determined by the direction of the circular magnetic field, i.e., the helices have opposite signs in the different halves of the layer. Thus, so long as the TM-state layer is in the interior of the sample, it has no effect on the magnitude of the longitudinal magnetic field in the aperture; it appears, however, that the longitudinal magnetic field must appreciably exceed the external field in the middle of the layer where the circular magnetic field is close to zero. The emergence of the layer to the sample surface decreases one of its parts and hence leads to an effect of one sign or another.

The singularities that were observed in the dependence of H_i/H_c on H_e/H_c (Fig. 5) are of considerable interest. Taking into account the results of measuring the surface impedance (Fig. 6), we can assert that we deal with a phase transition in the TM-state layer. The fact that jumps are observed on the $H_i/H_c = f(H_e/H_c)$ curves for both increasing and decreasing magnetic field, as well as the presence of a marked hysteresis, indicate that this transition is not the beginning of the trivial destruction of the TM-state layer by a longitudinal magnetic field.

2. Paramagnetic effect in the presence of a transverse magnetic field.

Figure 9 shows a number of H_i/H_e curves vs. the transverse magnetic field $H_\perp$ at various values of the current through the sample and at fixed value of H_e; Fig. 10 shows similar curves for a fixed value of the current and variable H_e.

On the face of it, the curves look rather unexpected. Indeed, an increase in the transverse magnetic field causes destruction of the TM-state layer, and nonetheless the magnitude of the paramagnetic effect increases. To understand why H_i/H_e increases with $H_\perp$ let us consider the influence of the transverse field on the TM-state layer.

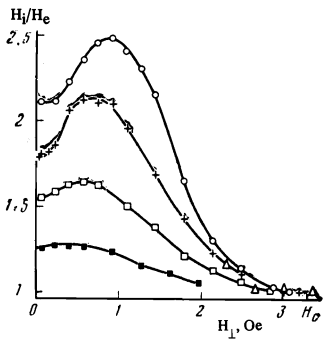

FIG. 9. Dependence of the magnitude of the paramagnetic effect on the transverse magnetic field. Sample In2, T = 3.375°K, $I_0 = 0.38\ I_c = 9.1$ A: O–H_e = 0.24 Oe, + –H_e = 0.73 Oe, □–H_e = 1.46 Oe, ■–H_e = 2.2 Oe; H_c = 3.3 Oe.

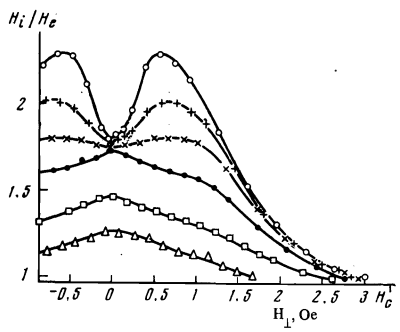

FIG. 10. Dependence of the magnitude of the paramagnetic effect on the transverse magnetic field. Sample In2, T = 3.375°K, H_e = 0.22 H_c = 0.73 Oe, O–I_0 = 8.5 Oe, +–I_0 = 11.7 A, X–I_0 = 16 A, □–I_0 = 106 A, Δ–I_0 = 160 A; I_c = 6.6 A.

It can be shown that application of a transverse magnetic field of magnitude $H_\perp$ redistributes the current in the layer of TM state in such a way that the magnetic field due to this current is distributed in the normal metal exactly like the magnetic field of a conductor carrying a current $I_L = cr_1(H_c^{12} - H_\perp^2)/H_c'$ and displaced relative to the center of the sample by $\delta r_1 = r_1 H_\perp / H_c'$ in that direction where the magnetic field of the current and the external magnetic field are oppositely directed (this is true so long as there exist no region of the intermediate state in the sample). It is readily seen that this distribution of current in the layer is the only one for which the total magnetic field in the normal metal immediately adjacent to the layer

$$H = H_I + H_\perp$$

is equal by magnitude to H_c' on the entire layer surface facing the normal metal (H_I is the current passing through the TM-state layer).

Let us now introduce a coordinate system with the origin at the center of the sample, the positive direction of X axis along the vector $\delta\mathbf{r}$, and the Y axis along $H_\perp$. In this frame the magnetic field in normal metal can be written in the form:

$$H(x)|_{y=0} = \frac{2I_L}{c(x-\delta r)} + \frac{2(I_0-I_L)(x^2-r_1^2)}{c(r_2^2-r_1^2)} - H_\perp.$$

The derivative

$$\frac{\partial H}{\partial x}\Big|_{x=r_1, y=0} = -2\frac{I_L}{c(r_1-\delta r)^2} + 4\frac{I_0-I_L}{c(r_2^2-r_1^2)}.$$

At

$$\frac{I_0}{I_c'} < \frac{H_c'+H_\perp}{H_c'-H_\perp}\left[\frac{r_2}{r_1} + \frac{r_1}{r_2} - 2\frac{r_1}{r_2}\frac{H_\perp}{H_c'}\left(2 - \frac{H_\perp}{H_c'}\right)\right]$$

we have $\partial H/\partial x < 0$; this means that the magnetic field, which is equal to H_c' on the boundary of the TM-state layer, decreases as we go deeper into the normal metal, i.e., there must exist a region of intermediate state in the normal metal. It is extremely difficult to exactly calculate the intermediate-state structure for this case. A crude sketch of this structure is shown in Fig. 11. The superconducting as well as the normal layers in the presence of a longitudinal magnetic field are likely to be stretched along the current, as is the case in solid cylindrical samples when their superconductivity is destroyed by current in the presence of a longitudinal magnetic field.[9] The shape of intersection of the layers with the XY plane is determined by the direction of the total transverse field. Thus, the domains, both superconductive and normal, are shaped like more or less distorted cylinders stretched along the current; such a structure is dynamical, and the direction of motion of the domain boundaries at various spots is shown by arrows in Fig. 11.

This motion of the domains apparently must lead to transport of the longitudinal magnetic flux encased in the normal layers into the aperture of the sample. It is this mechanism that causes the increase of the longitudinal magnetic field in the aperture when a transverse field is applied. The resulting value of the longitudinal field in the aperture is dictated by the balance between the rate of "pumping" the magnetic field by the motion of

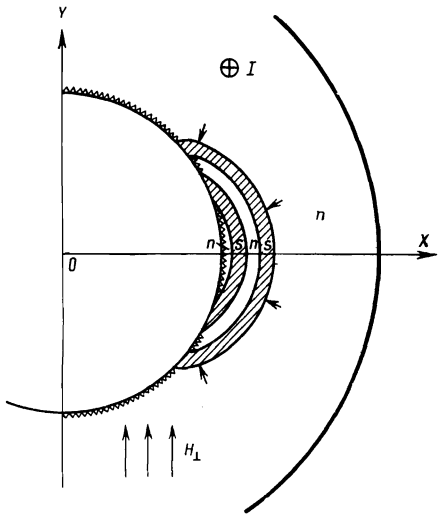

FIG. 11. Structure of the intermediate state in a hollow cylindrical current-carrying sample placed in external longitudinal and transverse magnetic fields. s and n are, respectively, the superconducting and normal regions, the toothed line shows the TM-state layer, and the small arrows indicate the direction of motion of domains.

superconducting layers and the rate of "leakage" of the magnetic field through the TM-state layer. An increase in the transverse magnetic field causes a growth of the region of intermediate state, but at the same time the superconducting properties of the TM-state layer weaken, i.e., the leakage rate of the magnetic field through the layer must increase. The competition of these two effects brings about the formation of a maximum in the dependence of H_i/H_e on $H_\perp$ (Figs. 9 and 10). An increase of the current through the sample reduces quickly the size of the intermediate-state region. Moreover, an increase of the current must augment the resistance of the TM-state layer, i.e., it must speed up the magnetic leakage out of the sample aperture; the proper paramagnetism of the TM-state layer decays too (see Fig. 8, b). All these effects jointly account for the sharp fall-off of the maxima in Fig. 10 as the sample current increases. An increase of the longitudinal magnetic field at a fixed current is likely to produce the same effect as an increase of the sample current, since in this case the characteristic unit for current I_c' falls off like $(H_c^2 - H_e^2)^{1/2}$.

Thus, the picture of the paramagnetic effect in hollow cylindrical samples in a transverse magnetic field somewhat resembles the same effect in solid cylindrical samples without a transverse magnetic field.[9] In both cases the pumping of the magnetic flux into the sample is due to the motion of superconducting layers, and the leakage occurs through a TM-state layer. The difference is that in the solid cylindrical samples the periods of leakage and pumping are separated in time, whereas in the case of a hollow sample in a transverse field both pumping and leakage occur simultaneously, although in different zones of the sample.

In conclusion I wish to express my deep gratitude to Yu. V. Shavrin for his useful advice on numerous occasions and his constant attention to the work; and to A. F. Andreev and W. Bestgen for their fruitful discussions.

[1] K. Steiner and H. Schoeneck, Phys. Z. **44**, 346 (1943). K. Steiner, Z. Naturforsch. **4a**, 271 (1949).
[2] H. Meissner, Phys. Rev. **101**, 1660 (1956).
[3] I. L. Landau and Yu. V. Shavrin, ZhETF Pis. Red. **10**, 192 (1969) [JETP Lett. **10**, 121 (1969)].
[4] I. L. Landau and Yu. V. Shavrin, ibid. **15**, 88 (1972) [**15**, 59 (1972)].
[5] A. F. Andreev and P. Tekel', Zh. Eksp. Teor. Fiz. **62**, 1540 (1972) [Sov. Phys.-JETP **35**, 807 (1972)].
[6] A. F. Andreev and W. Bestgen, ibid. **64**, 1865 (1973) [**37**, 942 (1973)].
[7] H. Meissner, Phys. Rev. **97**, 1627 (1955).
[8] C. Gorter, Physica **23**, 45 (1957).
[9] I. L. Landau, Zh. Eksp. Teor. Fiz. **64**, 557 (1973) [Sov. Phys.-JETP **37**, 285 (1973)].
[10] B. P. Peregud, Prib. Tekh. Eksp., No. 3, 64 (1957).
[11] M. A. R. LeBlane, B. C. Belanger, and R. M. Fieding, Phys. Rev. Lett. **14**, 704 (1965); B. C. Belanger and M. A. R. LeBlane, Appl. Phys. Lett. **10**, 298 (1967).
[12] F. F. Ternovskiĭ, Zh. Eksp. Teor. Fiz. **60**, 1790–1803 (1971) [Sov. Phys.-JETP **33**, 969 (1971)].
[13] V. Bestgen, ibid. **65**, 2097 (1973) [**38**, 1048 (1974)].
[14] A. F. Andreev, ZhETF Pis. Red. **10**, 453 (1969) [JETP Lett. **10**, 291 (1969)].

Translated by S. Luryi
33